Tracking and Mitigation of Chirp-Type Interference in GPS Receivers Using Adaptive Notch Filters

Arif, S., Coskun, A. and Kale, I.

This is a copy of the author’s accepted version of a paper subsequently published in the proceedings of Arif, S., Coskun, A. and Kale, I. 2020. Tracking and Mitigation of Chirp-Type Interference in GPS Receivers Using Adaptive Notch Filters. 2020 IEEE 63rd International Midwest Symposium on Circuits and Systems (MWSCAS). Springfield, MA, USA 09 - 12 Aug 2020 IEEE . https://doi.org/10.1109/MWSCAS48704.2020.9184659 .

The final published version will be available online at:

https://doi.org/10.1109/MWSCAS48704.2020.9184659

Chirp-Type Interference Tracking and Mitigation in GPS Receivers by Adaptive Notch Filters

Syed Waqas Arif, Adem Coskun and Izzet Kale
Applied DSP and VLSI Research Group
Department of Engineering
University of Westminster
waqas.arif@my.westminster.ac.uk, a.coskun@westminster.ac.uk, kalei@westminster.ac.uk

***Abstract*—Global Positioning System (GPS) receivers are extremely prone to intentional and unintentional interferences due to its weak signal power on the surface of the earth. Its functionality is severely affected and completely blinds the receivers from acquiring the GPS signal. This work presents a comparative and performance analysis of two different types of adaptive notch filtering algorithms for GPS specific application that is 1) Direct form 2nd Order and 2) Lattice-based Adaptive Notch Filters (ANF) for tracking and mitigation of Chirp-Like Interference. Three interference signals of interest are linear chirp, quadratic chirp and cubic chirp signal. Performance of each ANF algorithm is evaluated at the output of the acquisition module in term of search-grid SNR and Peak metric.**

Keywords—Anti-Jamming, Adaptive Notch Filter, GPS receivers, Chirp Interference.

I. INTRODUCTION

Global Positioning System (GPS) is in existence for more than four decades. It is most widely used satellite positioning constellation among existing Global Navigation Satellite System (GNSS). Commercial multi-constellation GNSS receivers have gained popularity in recent years. Whereas GPS provides world-wide coverage which makes it most favourable for research and development purposes for the satellite-based navigation and positioning receivers. Navigation signals transmitted by GNSS are modulated using Direct Sequence Spread Spectrum (DSSS) which provide built-in robustness to interference signal but only to some extent. The power level of the received GPS signal at receiver's RF end is of order 1×10^{-1} Watts and it is 20 dB below the thermal noise of the receiver. Due to extremely low received signal power level, the GNSS receivers are vulnerable to slighted of the interference in the in-band region of the useful signal spectrum. This effect of the interference signal on useful is very evident at the early stage of acquisition, known as Cross Ambiguity Function (CAF). Abnormities caused by interference signal are ripple through other operational blocks within the receiver, hence completely dysfunction receiver's ability to provide accurate Positioning, Velocity and Timing (PVT). Considering low GNSS signal power, this call for appropriate interference mitigation technique that is cost-effective and preserve the useful GNSS signal. Different types of interferences affect in different ways, hence distorting Corse-Acquisition (CA) code and CAF in the correlation process. There are numerous interference mitigation techniques which involve direct excision of interference signal based on Time-Frequency (TF) plane. Such techniques are adaptive frequency-domain filtering [1] and Time-Frequency Domain (TFD) [2]. But the drawback of these techniques is that it increases the computational load, which increases the hardware complexity of the GPS receivers despite the limited hardware resources and power available on-board. Various ANF algorithms have been implemented for interference suppression [3-5], however, most of the research focuses on excision of narrowband Continuous Wave Interference (CWI). ANF based techniques provided a cost-effective solution due to its low complexity and computational load [6] and proven to be very effective in excision of unwanted signal in the GNSS signals spectrum. Hence, ANF based algorithms have become very lucrative in the sense that it only requires two coefficients to realize second-order Infinite Impulse Response (IIR) ANF. In more challenging scenarios, where jamming signal's instantaneous frequency sweeps a range of several megahertz in few microseconds and corrupting entire GPS band. Such jamming signal is known as Chirp Signal (swept-frequency) and can be classified as linear-chirp, quadratic-chirp and cubic-chirp. The research work [7-8] demonstrates excision of linear swept frequency-chirp interference effectively via ANF using Auto-Regressive Moving-Average (ARMA) configuration. However, analysis of different ANF algorithms for tracking and mitigation of quadratic-chirp and cubic chirp within GNSS receivers is still far from being fully covered and this research addresses mitigation of other types of chirp interferences via lattice-based ANF and Direct Form second IIR ANF to enrich and broaden the investigation.

This paper is divided into five sections. Section II describes the modelling of the signals and system within an acquisition module. Section III discusses ANF algorithms based on the adaptation of notch centre frequency. Section IV demonstrates a simulation based results. Section V summarizes the conclusion.

II. SIGNAL AND SYSTEM MODEL

A. Chirp Interferences

A chirp signal is characterize by instantaneous variations of carrier frequency over frequency bandwidth known as sweep bandwidth B_c over one chirp period T_c. In this research main focus is chirp signal jamming tracking. Mathematical model of a linear chirp can be express as follow [9]:

$$j_{chir}\ [n] = \sqrt{2P_c}\cos\underbrace{(2\pi f_o nT_s + 2\pi u_c (nT_s)^2/2 + \emptyset_c)}_{\theta[n]} \quad (1)$$

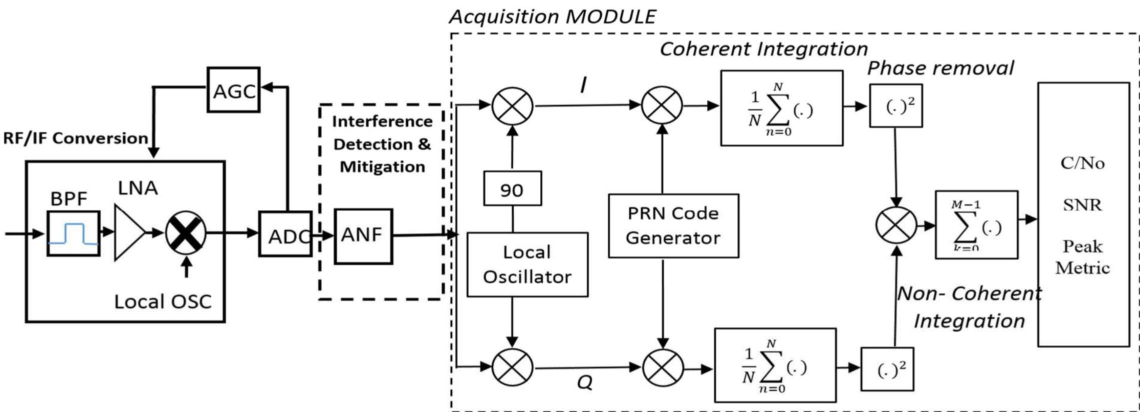

Figure 1. Generic RF/IF and Acquisition module of GPS receivers

Where P_c is chirp signal power, f_o is the initial frequency of sweep range, u_c is the chirp sweep rate as defined as B_c/T_c and $\emptyset_c$ is the initial chirp phase. Instantaneous angular frequency of the chirp signal is calculated by taking the first derivative of phase (2). Similarly, we can modify (1) to generate a non-linear chirp signal whose instantaneous frequency changes quadratic and cubically is expressed as in (3).

$$\frac{\partial}{\partial(nT_s)}(\theta[n]) = 2\pi f_o + 2\pi u_c n T_s \quad (2)$$

$$j_{chirp}[n] = \sqrt{2P_c}\cos\left(2\pi f_o n T_s + \frac{2\pi u_g (nT_s)^{1+p}}{1+p} + \emptyset_c\right) \quad (3)$$

$$u_g = B_c/\ T_c^p \quad (4)$$

Where p presents the order polynomial, for quadratic chirp and cubic chirp p equals 2 and 3 respectively and instantaneous angular frequency is given by (5)

$$\frac{\partial}{\partial(nT_s)}(\theta[n]) = 2\pi f_o + \frac{(1+p)\times 2\pi u_c (nT_s)^p}{1+p} \quad (5)$$

B. Received GPS Signal and Acquisition

The ideal GPS L1 signal with CWI at receiver front-end can be expressed as in (1) where $s_k[n]$ is transmitted signal by k^{th} satellite, $\eta[n]$ is the thermal noise level and $j_{chirp}[n]$ is the desired chirp interference signal.

$$r[n] = \sum_{k=1}^{N} s_k[n] + \eta[n] + j_{chirp}[n] \quad (6)$$

$$s[n] = \sqrt{2P_i} D_k[n-\tau_k] C_k[n-\tau_k] \cos(2\pi f_{L1+d} n T_s + \theta) \quad (7)$$

In (2) the P_i is the signal power, D_k is the navigation data bit of k^{th} satellite with a chip rate of 50 Hz, and C_k is coarse C/A code of k^{th} satellite running at a chip rate of 1.023MHz and τ_k is the code phase delay of k^{th} satellite. Frequency parameter f_{L1+d} represents the L1 carrier frequency with a Doppler shift of f_d (where the sum of these two frequency components results in $f_{L1+d} = f_{L1} \pm f_d = 1575.42MHz \pm f_d$). Next step is the acquisition of the GPS L1 signal and one of the most critical stages for any GNSS receivers. In Fig .1 a simplified scheme of initial stages of GNSS receivers is shown. GPS L1 signal is filtered and down-converted to Intermediate Frequency (IF) and equivalent filter bandwidth equals to B_{IF}.Then IF signal transforms into a sequence of samples by Analog-to-Digital Converter (ADC) control by Automatic Gain Control (AGC). At IF section received signal is represented by (8). Parallel code search based acquisition scheme is employed here, in which all the local C/A codes are searched simultaneously. In parallel code search, the

$$r_{IF}[n] = \sum_{k=1}^{N} s_{kIF}[n] + \eta_{IF}[n] + j_{chirpIF}[n] \quad (8)$$

fourier transform of the local C/A code $c_L[n]$ is performed and then the complex conjugate of the Fourier transform of the C/A code is multiplied with the Fourier transform of the received signal $r_{IF}[n]$. The resultant output is then transformed back into the time domain by the inverse transform. The final output thus represents the correlation between the received signal and the local C/A code known as Cross Ambiguity Function (CAF) as in (9). In an ideal scenario after evaluation of CAF, it should present with well

$$S(\tau_0, f_d) = \left|\frac{1}{N}\sum_{n=0}^{N-1} r_{IF}[n] c_L[n-\tau_0] e^{-j2\pi f_d}\right|^2 \quad (9)$$

define a sharp peak and the values of the peak corresponds to the value of τ_0 *and* f_d which matches delay and Doppler frequency of the satellite in space. Fig.2 shows the simulations of three chirp jamming signals and GPS L1 signal with a sampling frequency of 5 MHz.

C. Performance Metrics

The performance of the GPS acquisition systems is evaluated using CAF which in the discrete-time domain, can be defined as (9) and the Signal-to-Noise Ratio (SNR) in CAF is calculated by (10). The SNR is simply evaluated by dividing the difference of maximum correlation peak and mean noise

$$SNR(dB) = 10log\left[\frac{\max[S(\tau_0,f_d)] - mean[S(\tau_0,f_d)]}{s.t.d[S(\tau_0,f_d)]}\right] \quad (10)$$

of the search space by the standard deviation of the search space[11]. Second performance matric that is used is called search-grid peak metric α_{peak}, which is simply ration between the highest peak and second high peak in search-grid as in (11). If the α_{peak} value is above 2 it means received signal $r_{IF}[n]$ is easily acquirable[11].

$$\alpha_{peak} = \frac{|\max[S(\tau_0,f_d)]|}{second-max-pea\ \ (|S_{noise\ floor}|)} > 2 \quad (11)$$

III. ADAPTIVE NOTCH FILTERS

There is an extensive literature on the detection and mitigation of CWI in GNSS. The ANF is the evolution of the notch central frequency with passband frequency response remain constant but create a narrow notch at corresponding interference frequency and excise the interference signal. Two

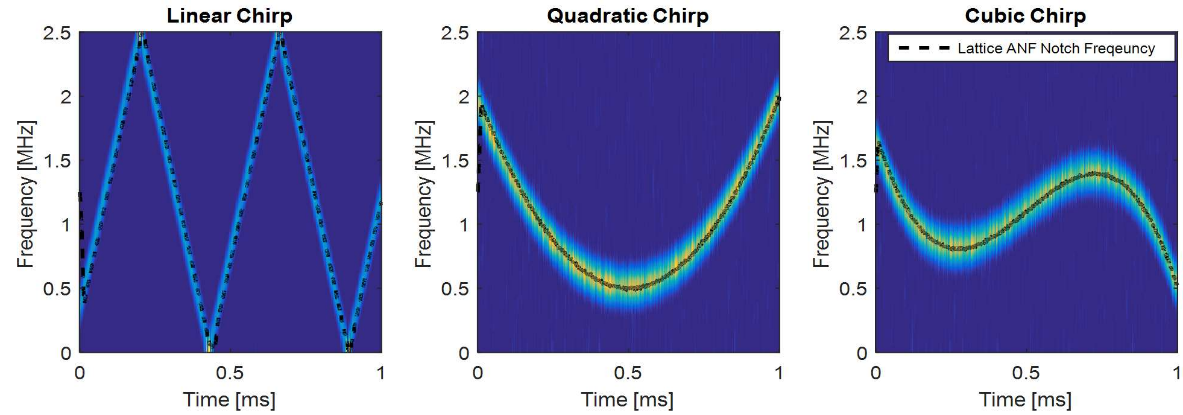

Figure 2. Time-Frequency representation of GPS L1 signal interfered by linear, quadratic and cubic Chirp over 1ms (1 complete C/A code). Black dashed line represents the instantaneous frequency of lattice based ANF.

candidates for ANF algorithms are modelled and investigated. Firstly , A lattice based ANF [10] and other on 2nd order direct form IIR ANF [6]. In an adaptive IIR lattice structure the notch filter transfer function from input $x_{in}[n]$ to notch output $y_L[n]$ is expressed as by (12)

$$H_L(z) = \frac{1+\rho}{2}\frac{1-2\beta[n]z^{-1}+z^{-2}}{1-\beta[n](1+\rho)z^{-1}+\rho z^{-2}} \quad (12)$$

$$\beta[n] = \beta[n-1] - \mu.\, y_L[n](1-\rho)x[n-1] \quad (13)$$

where β is the notch centre frequency parameter and ρ is notch bandwidth parameter of the lattice notch filter. Update equation for β is given by (13), where μ is fixed step-size and kept fixed rather than time-varying step-size as in [10] to simplify realisation of algorithm. Direct form 2nd ANF is modelled as given in [6]. The Normalized Least Mean Square (NLMS) algorithm is utilized to update the location of the instantaneous frequency of chirp interference. The transfer function of the notch filter is given as follows

$$H_{notch}(z) = \frac{(1-2Real(z_0)z^{-1}+|z_0|^2z^{-2})}{1-2k_\alpha Real(z_0)z^{-1}+{k_\alpha}^2|z_0|^2z^{-2}} \quad (14)$$

where k_α is the notch bandwidth parameter and z_0 is the notch location on the unit circle corresponds to instantaneous frequency of chirp signal. Output of the ANF is minimized by taking the derivative of (14) with respect to the parameter z_0. The expression of the stochastic gradient is given by

$$grad(C[n]) = -4x_0[n](z_0[n-1]x_e[n-2] - x_e[n-1]) \quad (15)$$

where $x_0[n]$ is the output of Auto-Regressive (AR) is part of the filter and $x_e[n]$ is the output of Moving-Average (MA) part of the filter [9] and the equation to update the zero of ANF becomes as follows

$$z_0[n] = z_0[n-1] + \mu_n \times x_0[n]grad(C[n]) \quad (16)$$

where μ_n normalized step-size. The performance of the both ANF is determined and dependent on notch bandwidth parameters (ρ & k_α) and fast convergence (μ & μ_n) capability. These parameters play influential role to track fast variations in frequency and needed to be tuned very carefully. Setting notch bandwidth parameters close to unity (very narrow notch) will preserve the useful signal but it will become difficult for ANF to tracking fast variation of instantaneous frequency of chirp interference, hence a good trade-off is required to successfully tracking frequency varying signal.

IV. Simulations

Three digital chirp interference signals are simulated according to definition of the parameters that are explained in section II and combined with simulated GPS L1 signal. A complete list of the parameters are given in table 1 for the simulation setup. Fig 1 shows time-frequency representation of the simulated GPS L1 signal added with chirp interference signals. Blacked dashed line shows the evolution of the notch centre frequency of lattice based ANF. It is assume generated sweep range of the chirp signal are bounded by pass-bandwidth of RF front-end. Also Jamming-to-Nosie Density (J/N_0) range kept is small (5dB to 15dB) to make sure minimal adjustments are required for the parameters of the both ANF without pushing ANF into unstable region. Along with that notch bandwidth parameter are kept same for both ANF which is 0.85, by doing so, both filter have same notch bandwidth and nor close to unity. Hence provide similar parameters to evaluate performance of both ANF. Tracking and converging performance of two ANF are shown in fig.3. From this simulation it is evident that the variance in the estimated frequency by direct form ANF is more visible near DC and Nyquist as shown by grey line in fig 3. On other hand variance of estimated frequency by Lattice ANF is small and more uniform in nature over wide range of frequency. Furthermore, table 2 lists the resulting values of the performance metrics discussed in section II. At the output of acquisition module values of SNR and α_{peak} are calculated for different power level of linear and quadratic chirp interference signal. Bold values in table 2 shows where

Table 1. Simulation Setup

Simulation Parameters		**Values**
GPS L1 IF signal	Sampling Frequency (F_s)	5MHz
	Intermediate Frequency (IF)	1.25Mhz
	Received Signal Power (P_i)	-160dBW
Acquisition	Front-end Bandwidth (B_{IF})	5MHz
	Coherent Integration Time	1ms
	Doppler bin size	125Hz
Lattice ANF	Step-size (μ)	0.01-0.03
	Notch bandwidth (ρ)	0.85
Direct Form ANF	Step-size (μ_n)	0.01-0.025
	Notch bandwidth (k_α)	0.85

Table 2 : SNR and α_{peak} values at the output of Acquisition module

	Lattice ANF				Direct Form 2nd order ANF			
	Linear Chirp		Quadratic Chirp		Linear Chirp		Quadratic Chirp	
J/N_0(dB)	**SNR(dB)**	**α_{peak}**	**SNR(dB)**	**α_{peak}**	**SNR(dB)**	**α_{peak}**	**SNR(dB)**	**α_{peak}**
5	13.87	2.71	14.17	2.87	12.51	2.23	12.73	2.33
8	13.18	2.53	12.96	2.39	11.41	2.01	11.10	2.09
12	12.73	2.31	10.78	2.1	10.47	**1.94**	**9.31**	**1.54**
15	11.93	2.07	10.19	**1.89**	**8.91**	**1.37**	**8.46**	**1.37**

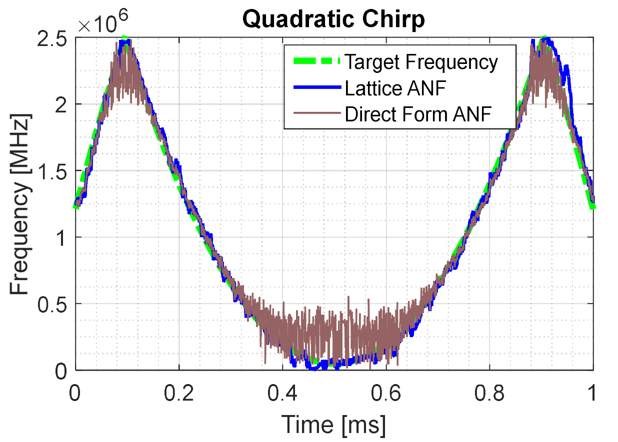

Figure 3. Tracking and converges performance of lattice ANF shown by blue line and Direct Form ANF shown by grey. Green thick dash line represents the target frequency

each of the ANF failed to acquire signal and both SNR and α_{peak} values degrade more prominently for direct form ANF. As long as the SNR at the output of acquisition module is more than 10 dB, the GPS L1 signal is acquirable by employing multiple non-coherent integration over period of 1msec and if the peak value is 2 or more, means useful signal is more prominent in noise bed of the search-grid.

V. CONCLUSION

In this research article, three different types of chirp jamming signal, the linear, quadratic and cubic chirps are modelled and analysed. Using a practical simulation models, a complete GPS L1 IF signal and acquisition module is simulated. Both ANF structures are compared and assess in terms of tracking, variance, SNR and α_{peak} for GPS L1 signal. Simulation results prove that the lattice structure shows superior performance in term tracking ability and SNR at the output of the acquisition module. Experiments results shows lattice based ANF is an excellent candidate for tracking quadratic and cubic chirps for GPS specific application and for cubic chirp further analysis being carried out in term of performance metrics. This research is being expanded further, it is well known fact that 90% of GPS L1 signal power is in the main lobe (2MHz in bandwidth) and furthermore if some (12-18%) portion of main lobe is discarded even than GPS L1 is can be acquired, this means ANF have to excise interference signal mainly from the main lobe and required less processing time. Hence work is being carried on to find right trade-off between the quality of interference excision and computational complexity of the system.

REFERENCES

[1] P. Wang, E. Cetin, A. G. Dempster, Y. Wang, and S. Wu, 'Improved Characterization of GNSS Jammers Using Short-Term Time-Frequency Rényi Entropy', *IEEE Transactions on Aerospace and Electronic Systems*, vol. 54, no. 4, pp. 1918–1930, Aug. 2018

[2] M. G. Amin, D. Borio, Y. D. Zhang, and L. Galleani, 'Time-Frequency Analysis for GNSSs: From interference mitigation to system monitoring', *IEEE Signal Processing Magazine*, vol. 34, no. 5, pp. 85–95, Sep. 2017

[3] L. Musumeci, J. T. Curran, and F. Dovis, "A Comparative Analysis of Adaptive Notch Filtering and Wavelet Mitigation against Jammers Interference," *ION*, vol. 63, no. 4, pp. 533–550, Dec. 2016.

[4] Q. Lv and H. Qin, 'A Novel Algorithm for Adaptive Notch Filter to Detect and Mitigate the CWI for GNSS Receivers', in *2018 IEEE 3rd International Conference on Signal and Image Processing (ICSIP)*, Jul. 2018, pp. 444–451

[5] E. Falletti, M. T. Gamba, and M. Pini, 'Design and Analysis of Activation Strategies for Adaptive Notch Filters to Suppress GNSS Jamming', *IEEE Transactions on Aerospace and Electronic Systems*, pp. 1–1, 2020,

[6] D. Borio, L. Camoriano, and L. L. Presti, "Two-Pole and Multi-Pole Notch Filters: a Computationally Effective Solution for Interference Detection and Mitigation," in *2007 7th International Conference on ITS Telecommunications*, 2007, pp. 1–6.

[7] Y.-E. Chen, Y.-R. Chien, and H.-W. Tsao, 'Chirp-Like Jamming Mitigation for GPS Receivers Using Wavelet-Packet-Transform-Assisted Adaptive Filters', in *2016 International Computer Symposium (ICS)*, Dec. 2016, pp. 458–461

[8] D. Borio, 'Swept GNSS jamming mitigation through pulse blanking', in *2016 European Navigation Conference (ENC)*, May 2016, pp. 1–8

[9] J. R. Klauder, A. C. Price, S. Darlington, and W. J. Albersheim, 'The theory and design of chirp radars', *The Bell System Technical Journal*, vol. 39, no. 4, pp. 745–808, Jul. 1960

[10] Y. R. Chien, "Design of GPS Anti-Jamming Systems Using Adaptive Notch Filters," *IEEE Systems Journal*, vol. 9, no. 2, pp. 451–460, Jun. 2015.

[11] S. W. Arif, A. Coskun, and I. Kale, 'A Fully Adaptive Lattice-based Notch Filter for Mitigation of Interference in GPS', in *2019 15th Conference on Ph.D Research in Microelectronics and Electronics (PRIME)*, Jul. 2019, pp. 217–220